Chinese Chemical Letters 31 (2020) 992–995

Contents lists available at ScienceDirect

Chinese Chemical Letters

journal homepage: www.elsevier.com/locate/cclet

Communication

Highly efficient catalytic performances of nitro compounds *via* hierarchical PdNPs-loaded MXene/polymer nanocomposites synthesized through electrospinning strategy for wastewater treatment

Juanjuan Yin[a,b], Fangke Zhan[b], Tifeng Jiao[a,b,*], Huizhen Deng[b], Guodong Zou[a], Zhenhua Bai[c], Qingrui Zhang[b,**], Qiuming Peng[a,**]

[a] State Key Laboratory of Metastable Materials Science and Technology, Yanshan University, Qinhuangdao 066004, China
[b] Hebei Key Laboratory of Applied Chemistry, School of Environmental and Chemical Engineering, Yanshan University, Qinhuangdao 066004, China
[c] National Engineering Research Center for Equipment and Technology of Cold Strip Rolling, Yanshan University, Qinhuangdao 066004, China

ARTICLE INFO

Article history:
Received 20 July 2019
Received in revised form 3 August 2019
Accepted 5 August 2019
Available online 28 August 2019

Keywords:
Electrospinning
MXene sheet
Self-reduction
Palladium nanoparticle
Catalyst

ABSTRACT

The problem of water pollution has become increasingly serious, and it has already threatened the survival of mankind and has become an obstacle to the healthy development of human health. Here, we prepared a novel polyvinyl alcohol (PVA)/polyacrylic acid (PAA)/MXene fiber membrane by electrospinning. After heat treatment of film and subsequent modification with Pd nanoparticles, PVA/PAA/MXene@PdNPs composite nanofiber membrane with high specific surface area and excellent catalytic performance was finally prepared. The uniform distribution of MXene sheets in the composite fiber membrane not only solves the problem that the MXene sheet is not easy to be monolayerized, but also can grow the self-reduced Pd nanoparticles on the MXene sheets. In addition, the composite nanofiber membrane exhibits excellent catalytic ability and cycle stability for 4-nitrophenol (4-NP) and 2-nitrophenol (2-NA), providing new strategy for the study of catalytic composite materials related to degradation of wastewater.

In recent years, the problem of water pollution has become a hot spot of concern. The sewage treatment has also become the research focus. Among them, the main sources of sewage are domestic sewage and chemical dye wastewater. Nitrophenol is well known as the most common organic pollutant in industrial and agricultural wastewater [1]. At present, various methods for removing them have been developed, such as photocatalytic degradation [2], adsorption [3], microbial degradation [4], nitro reduction [5], microwave-assisted catalytic oxidation [6], and electrocoagulation [7]. However, considering the conditions such as energy saving, safe operation, and avoidance of use of an organic solvent, a method for converting 4-NP to 4-AP in an aqueous solution under mild conditions is urgently needed to develop.

In the past few decades, nanotechnology has developed rapidly in various fields, especially precious metal nanoparticles. Due to the excellent catalytic performance of noble metal nanoparticles, they have been widely concerned in the world, such as gold, palladium, *etc.* [8,9]. However, since the palladium nanoparticles have high surface energy, resulting in instability and easy aggregation of the palladium nanoparticles, the catalytic performance and catalytic efficiency of the palladium nanoparticles are suppressed [10]. According to research, loading particles onto a carrier substrate [11–13] is one of the effective methods for solving the aggregation of metal particles. Recently, a variety of different palladium based catalysts have been reported. Mourdikoudis *et al.* prepared highly porous and hydrophobic palladium nanodendrites by a one-step process, and palladium nanodendrites exhibited excellent performance of recyclable catalysts [14]. Zhao *et al.* proposed a convenient, time-saving, economical, and sustainable method for immobilizing Pd NP on filter paper by PEI-mediated *in situ* reduction, and this material is reusable in the reduction conversion of Cr(VI) to Cr(III) and 4-nitrophenol to 4-aminophenol. [15]. Wang *et al.* successfully prepared a polyethyleneimine/

* Corresponding author at: State Key Laboratory of Metastable Materials Science and Technology, Yanshan University, Qinhuangdao 066004, China.
** Corresponding authors.
E-mail addresses: tfjiao@ysu.edu.cn (T. Jiao), zhangqr@ysu.edu.cn (Q. Zhang), pengqiuming@ysu.edu.cn (Q. Peng).

polycaprolactone composite fiber membrane decorated with palladium nanoparticles by electrospinning method, which has high and recoverable catalytic performance for nitro compounds [10]. Therefore, electrospun fibers can be used as an ideal carrier for metal nanoparticles. MXene is a new layered two-dimensional (2D) material with excellent surface area and excellent properties, providing a carrier substrate for the reduction of metal particles [16]. Huang *et al.* prepared a graded AgNP-loaded MXene/Fe_3O_4/polymer nanocomposite for enhanced catalytic performance [17]. However, MXene nanosheets are prone to aggregation in solution and are prone to oxidation, which has become an urgent challenge. Boota *et al.* prepared PPy/$Ti_3C_2T_x$ composites through modifying polypyrrole on the surface of MXene [18]. However, after the surface of the MXene sheet is modified, its self-reducing precious metal properties are masked.

In order to solve the above problems, we successfully synthesized PVA/PAA/MXene@PdNPs functional nanocomposites by electrospinning technology. Electrospinning is well known as a simple and effective method for the direct and continuous preparation of polymer nanofibers [19,20]. The prepared electrospun fibers have unique characteristics such as specific surface area and high porosity [21], which can be widely used in adsorption [22], catalysis and filtration [23–25]. At the same time, PVA and PAA are water-soluble and environmentally friendly materials, which are non-polluting and easy to degrade. In addition, PVA/PAA/MXene@PdNPs nanofibers synthesized by electrospinning technology not only make MXene sheets evenly distributed on the spinning, reduce the aggregation of MXene in solution, but also provide a substrate for the reduction of Pd nanoparticles. In this work, the structural characterization and performance tests of the PVA/PAA/MXene@PdNPs composite nanofibers show that the composite fiber material behaves excellent catalytic reduction performance of nitro compounds such as 2-nitrophenol (2-NA) and 4-nitrophenol (4-NP), which means that the new PVA/PAA/MXene@PdNPs composite nanofibers provide a new strategy in future wastewater treatment.

In this study, as shown in Fig. 1, the stratified PdNPs-loaded MXene/polymer nanocomposites synthesized by the electrospinning strategy have high catalytic performance for wastewater-treated nitro compounds. First, a solution of the MXene flake dispersion was separately added to the PVA and PAA solutions. Next, the two solutions of PVA and PAA were uniformly mixed with each other to be spun. Finally, PVA/PAA/MXene composite nanofiber membranes were prepared by electrospinning technology. After the composite fiber membrane was dried, it was placed in a $PdCl_2$ solution with an appropriate time. Then, the membrane was washed with ethanol and ultrapure water for several times and dried to finally obtain a PVA/PAA/MXene@PdNPs composite nanofiber membrane. Finally, the catalytic activity of PVA/PAA/MXene@PdNPs composite nanofiber membranes for 2-NA and 4-NP was studied. It is worth noting that since the electrons in the low-priced titanium in MXene are oxidized to a high valence state, the electrons of the Pd^{2+} ion are reduced to PdNPs. In addition, with the addition of MXene sheets and PdNPs, the PVA/PAA/MXene@PdNPs composite fiber film with higher specific surface area was obtained, and the specific surface area increased from 9.63 m^2/g to 13.48 m^2/g, as shown in Table S1 (Supporting information).

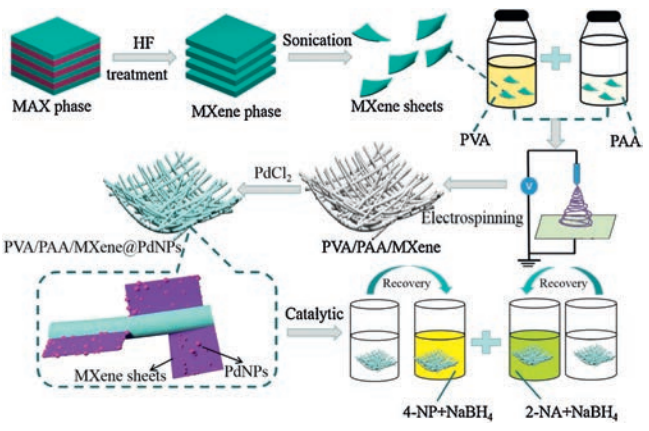

Fig. 1. Schematic illustration of preparation process of the obtianed composite fibers.

X-ray diffraction (XRD) data is used to reflect strong affiliations in composite nanofibers. Fig. S1a (Supporting information) shows the XRD pattern of MXene powder, PVA/PAA nanofibers, PVA/PAA/MXene composite nanofibers and PVA/PAA/MXene@PdNPs composite nanofibers. The curve of MXene powder clearly indicates that the characteristic peaks are at $2\theta = 8.90°$, 18.24° and 27.65°, which are assigned to the (002), (006) and (008) crystal faces [26], respectively. XRD peaks were observed at 19.58° (PVA/PAA) and 20.24° (PVA/PAA/MXene), indicating the addition of MXene flakes to the composite nanofiber layer. In addition, the XRD inset shows the characteristic peaks of PdNPs corresponding to (111), (200) and (220) planes, which further confirms the successful loading of PdNPs [27].

The thermal stability of different composite nanofibers was measured by TG, as shown in Fig. S1b (Supporting information). A small weight loss was observed at 180 °C, indicating evaporation of moisture in the nanofiber material. Further, the weight loss is remarkably increased due to thermal decomposition of the carbon chain between 250 °C and 450 °C. When the temperature reached 480 °C, the weight loss value of the nanofibers remained constant. Therefore, the heat loss rates of PVA/PAA, PVA/PAA/MXene and PVA/PAA/MXene@PdNPs spinning films were 73.15%, 67.30% and 57.1%, respectively. The results show that the PVA/PAA/MXene spinning fiber has relatively less heat loss due to the successful addition of MXene sheet, while the PVA/PAA/MXene@PdNPs spinning film has the least heat loss of the spinning fiber, indicating that MXene nanosheets and Pd nanoparticles were successfully anchored in the obtained fibers.

Next, the morphology of PVA/PAA/MXene@PdNPs composite nanofibers was characterized by SEM, as shown in Fig. 2. Figs. 2a–c depict the SEM structures of PVA/PAA, PVA/PAA/MXene and PVA/PAA/MXene@PdNPs, respectively. The PVA/PAA nanofibers exhibit a relatively uniform filament shape with an average diameter of about 500 nm. After the addition of MXene sheets, the morphology of the prepared PVA/PAA/MXene composite nanofibers changed. As shown in Fig. 2b, the MXene sheets were uniformly distributed on the spun fibers, indicating that the MXene sheets were successfully embedded in the fibers. Finally, the PVA/PAA/MXene membrane was immersed in $PdCl_2$ solution to obtain PVA/PAA/MXene composite nanofibers loaded with PdNPs, as shown in Fig. 2c. By mapping the elements in the SEM, as shown in Figs. 2d–g, the images of PVA/PAA/MXene@PdNPs clearly show the existence of carbon, oxygen, titanium and palladium elements, further proving the successful loading of PdNPs. In order to further analyze the structure of the prepared PVA/PAA/MXene@PdNPs composite nanofibers. Fig. 2h shows that the plane spacing d (111) = 0.240 nm of the lattice data can fully prove that PdNPs were successfully prepared, which is consistent with the results expressed in XRD.

We used XPS technology to study the elemental composition and Pd^{2+} reduction level on the surface of PVA/PAA/MXene@PdNPs composite nanofibers (Fig. 3). Figs. 3b–d represent characteristic peaks of C 1s, O 1s and Pd 3d, respectively. The XPS spectrum of Pd 3d shows a double peak with a binding energy of 337.5 eV and 343.3 eV, corresponding to the Pd $3d_{5/2}$ and Pd $3d_{3/2}$ components of the metal Pd(0) state, which confirms the presence of metal Pd [28–30]. In addition, we analyzed the oxygen and carbon elements.

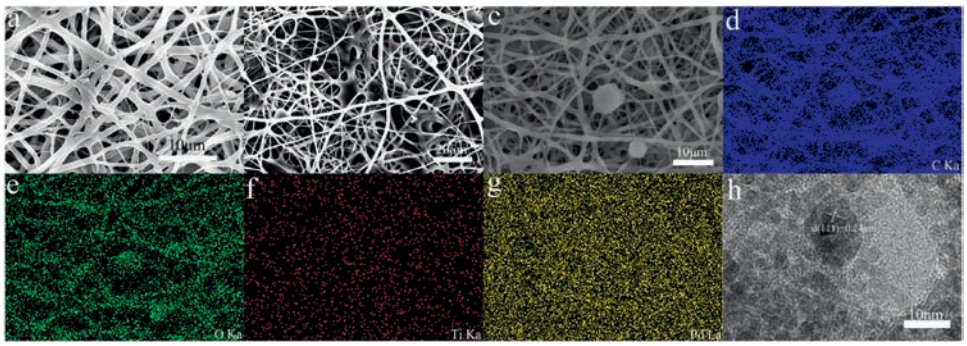

Fig. 2. SEM images of PVA/PAA nanofibers (a), PVA/PAA/MXene nanofibers (b), PVA/PAA/MXene@PdNPs nanofibers (c), C/O/Ti/Pd elemental mapping (d–g), and high-resolution TEM images of Pd nanoparticles (h).

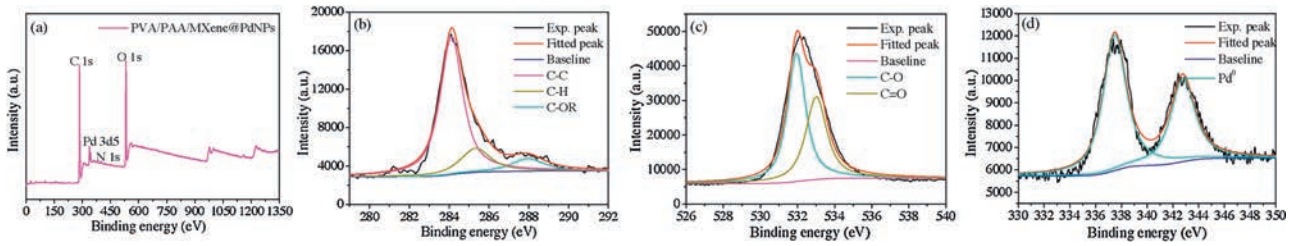

Fig. 3. XPS profiles of the PVA/PAA/MXene@PdNP nanofibers (a) and elemental mappings: C 1s (b), O 1s (c), and Pd 3d (d).

The peaks appearing at 284.7 eV, 285.8 eV and 288.8 eV are respectively the peaks of C 1s, representing C–C, C–H and C–OR. Then, the peaks at 532.1 eV and 532.8 eV are respectively the peaks of O 1s, representing C–O bonds and C=O bonds [31].

Next, as a new catalyst, the obtained PVA/PAA/MXene@PdNPs composite nanofibers were used to study the catalytic performances of the nitro compound (4-NP, 2-NA). As shown in Fig. 4a, the color of 4-NP solution is pale yellow in neutral and acid environments. Under the influence of $NaBH_4$ at room temperature, the color of the solution immediately changed from pale yellow to bright yellow because of the formation of *p*-nitrophenol ions, and the absorption peak moved from 317 nm to 402 nm [32]. As the reaction progressed, the absorption peak of 4-AP gradually appeared near 295 nm, and meanwhile the solution was almost colorless. When PVA/PAA/MXene@PdNPs composite nanofibers were added, the peak of 4-NP gradually decreased at 402 nm over time, indicating that 4-NP was continuously catalyzed (Fig. 4b) [33]. It is worth mentioning that the concentration of $NaBH_4$ is negligible throughout the reaction due to the large initial concentration of $NaBH_4$, and the entire process of catalyzing

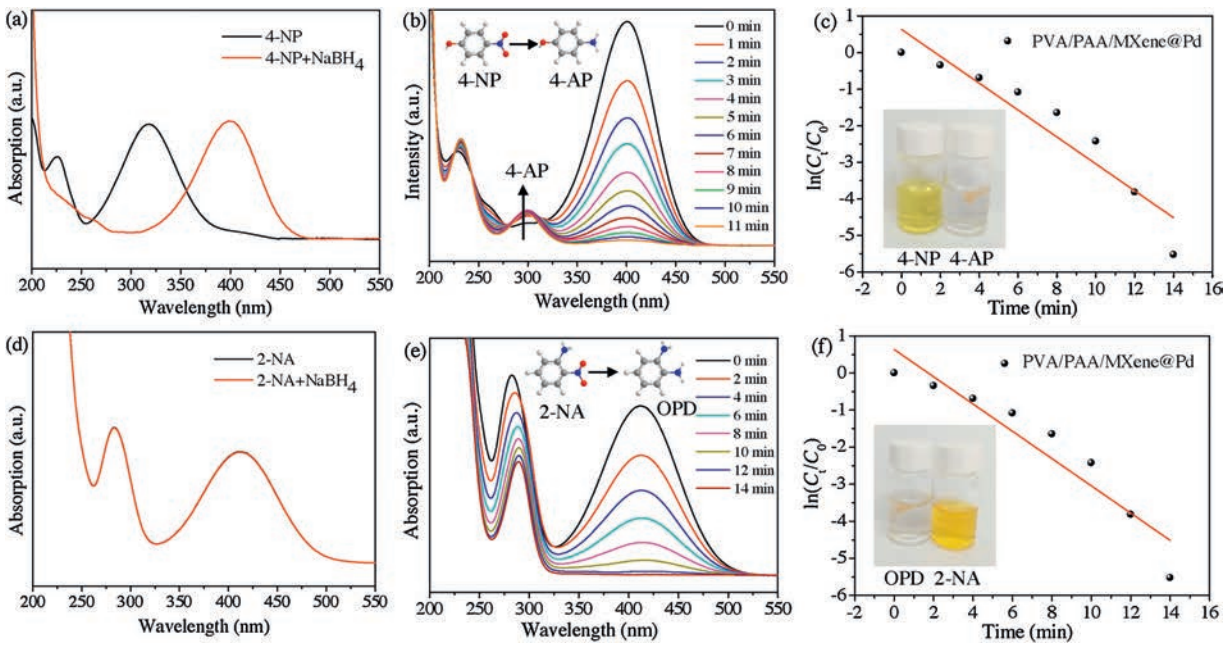

Fig. 4. UV–vis spectra of 4-NP (a) and 2-NA (d) before and after adding $NaBH_4$ aqueous solution; catalytic reduction of 4-NP or 2-NA with PVA/PAA/MXene@PdNPs composite nanofibers (b,e); and relationship between $\ln(C_t/C_0)$ and the reaction time (t) of composite nanofiber catalyst (c,f).

4-NP can be regarded as a *quasi*-first-order reaction. As shown in Fig. 4c, the linear relationship of $\ln(C_t/C_0)$-t in the catalytic reaction indicates that the catalytic reaction is a *pseudo* first-order reaction (C_t represents the concentration at a certain moment, C_0 represents the initial concentration and t indicates the reaction time). The kinetic constant (k) of PVA/PAA/MXene@PdNPs composite nanofibers for catalytic reduction of *p*-nitrophenol was 0.367 min^{-1}. The results show that PVA/PAA/MXene@PdNPs composite nanofibers has good catalytic activity for 4-NP.

To further evaluate the catalytic activity of PVA/PAA/MXene@PdNPs composite nanofibers, we also performed experiments to catalyze 2-NA reactions. Similarly, the color of the mixture of 2-NA and $NaBH_4$ remained steady for 24 h in the absence of a catalyst, the color of 2-NA exhibited a bright yellow color [34–38], and the position of the absorption peak of 2-NA was 415 nm. After the addition of $NaBH_4$, the position of the absorption peak of 2-NA is still 415 nm, as shown in Fig. 4d. After adding appropriate amount of PVA/PAA/MXene@PdNPs composite fiber, the catalytic reaction was completed in 15 min, which proved that the process of composite fiber catalyzing 2-NA exhibited very obvious effect, as shown in Fig. 4e. It is similar that the catalytic reaction of PVA/PAA/MXene@PdNPs composite nanofibers to 2-NA can also be considered a *quasi*-first-order reaction (Fig. 4f). The kinetic constant (k) of PVA/PAA/MXene@PdNPs composite nanofibers for catalytic reduction of *o*-nitroaniline was 0.331 min^{-1}, which proved that the composite has good catalytic activity for 2-NA. In addition, the catalytic efficiencies of the composite fiber membranes PVA/PAA/MXene@PdNPs for 4-NP and 2-NA were 94% and 90%, respectively after 8 reuse cycles, as shown in Fig. S2 (Supporting information), demonstrating well stability and wide reuse applications. Thus, present obtained PVA/PAA/MXene@PdNPs composite nanofiber materials seemed to be an excellent catalyst for degrading dyes, which provided new idea for design of catalytic materials and self-assembled composites in the future [39–45].

In summary, we successfully designed and prepared a novel PVA/PAA/MXene@PdNPs composite nanofiber material with significant catalytic activity through the electrospinning technology and the self-reduction of Pd^{2+} ions by MXene flakes. After the use of MXene flakes, it provides a rich active linking site and sufficient space for the chemical modification of palladium, which is beneficial to the adhesion of palladium particles and reduces the aggregation of palladium during the reduction process. The PVA/PAA/MXene@PdNPs composite nanofibers exhibit excellent reactivity for the catalytic reaction of certain nitro compounds (such as 2-NA and 4-NP) due to special structural characteristics of composite nanofibers and good catalytic activity of PdNPs. Therefore, present work not only provides new research clues for the preparation of composite materials loaded with metal particle, but also lays a new foundation for wastewater treatment. At the same time, it has extremely important and potential worth for environmental management and sustainable development of composite materials.

Acknowledgments

We greatly appreciate the financial supports of the National Natural Science Foundation of China (No. 21872119), Support Program for the Top Young Talents of Hebei Province, China Postdoctoral Science Foundation (No. 2015M580214) and Research Program of the College Science & Technology of Hebei Province (No. ZD2018091).

Appendix A. Supplementary data

Supplementary material related to this article can be found, in the online version, at doi:https://doi.org/10.1016/j.cclet.2019.08.047.

References

[1] Y.C. Chang, D.H. Chen, J. Hazard. Mater. 165 (2009) 664–669.
[2] M.S. Dieckmann, K.A. Gray, Water Res. 30 (1996) 1169–1183.
[3] E. Marais, T. Nyokong, J. Hazard. Mater. 152 (2008) 293–301.
[4] O.A. O'Connor, L.Y. Young, Environ. Toxicol. Chem. 8 (1989) 853–862.
[5] L. Zhang, S. Zheng, D.E. Kang, J.Y. Shin, et al., RSC Adv. 3 (2013) 4692–4703.
[6] L.L. Bo, Y.B. Zhang, X. Quan, et al., J. Hazard. Mater. 153 (2008) 1201–1206.
[7] N. Modirshahla, M.A. Behnajady, S. Mohammadi-Aghdam, J. Hazard. Mater. 154 (2008) 778–786.
[8] K. Esumi, R. Isono, T. Yoshimura, Langmuir 20 (2004) 237–243.
[9] M. Pérez-Lorenzo, J. Phys. Chem. Lett. 3 (2012) 167–174.
[10] C. Wang, J. Yin, S. Han, et al., Catalysts 9 (2019) 559.
[11] B. Domènech, M. Muñoz, D.N. Muraviev, J. Macanás, Nanoscale Res. Lett. 6 (2011) 406.
[12] Y. Lin, Y. Qiao, Y. Wang, et al., J. Mater. Chem. 22 (2012) 18314–18320.
[13] S. Hermans, V. Bruyr, M. Devillers, J. Mater. Chem. 22 (2012) 14479–14486.
[14] S. Mourdikoudis, V. Montes-García, S. Rodal-Cedeira, et al., Dalton Trans. 48 (2019) 3758–3767.
[15] Y. Zhao, L. Liu, D. Shi, et al., Nanoscale Adv. 1 (2019) 342–346.
[16] B. Anasori, M.R. Lukatskaya, Y. Gogotsi, et al., Nat. Rev. Mater. 2 (2017) 16098.
[17] X. Huang, R. Wang, T. Jiao, et al., ACS Omega 4 (2019) 897–1906.
[18] M. Boota, B. Anasori, Y. Gogotsi, et al., Adv. Mater. 28 (2016) 1517–1522.
[19] N. Bhardwaj, S.C. Kundu, Biotechnol. Adv. 28 (2010) 325–347.
[20] Z.M. Huang, Y.Z. Zhang, M. Kotaki, et al., Compos. Sci. Technol. 63 (2003) 2223–2253.
[21] M.I. Shariful, S.B. Sharif, J.J.L. Lee, et al., Carbohyd. Polym. 157 (2017) 57–64.
[22] R. Zhao, Y. Wang, X. Li, B. Sun, et al., ACS Appl. Mater. Inter. 7 (2015) 26649–26657.
[23] J.S. Ye, Z.T. Liu, C.C. Lai, et al., Chem. Eng. J. 283 (2016) 304–312.
[24] S. Jiang, H. Hou, S. Agarwal, et al., ACS Sustain. Chem. Eng. 4 (2016) 4797–4804.
[25] K.K. Li, T.F. Jiao, R.R. Xing, et al., Sci. China Mater. 61 (2018) 728–736.
[26] D.D. Sun, H.U. Qian-Ku, L.I. Zheng-Yang, et al., J. Synth. Cryst. 43 (2014) 2950–2956.
[27] J. Yin, L. Zhang, T. Jiao, et al., Nanomaterials 9 (2019) 1009.
[28] S.D. Yang, J. Dong, Z.H. Yao, et al., Sci. Rep. 4 (2014) 4501.
[29] Q.L. Zhu, F.Z. Song, Q.J. Wang, et al., J. Mater. Chem. A: Mater. Energy Sustain. 6 (2018) 5544–5549.
[30] Z. Jin, D. Nackashi, W. Lu, et al., Chem. Mater. 22 (2010) 5695–5699.
[31] X. Yang, L. Li, F. Yan, Chem. Lett. 39 (2010) 118–119.
[32] Y. Shi, X. Zhang, Y. Zhu, et al., RSC Adv. 6 (2016) 47966–47973.
[33] S.E. Baghbamidi, A. Hassankhani, E. Sanchooli, S.M. Sadeghzadeh, Appl. Organomet. Chem. 32 (2018) 4251.
[34] P.C. Chen, S.C. Chen, Comput. Chem. 26 (2002) 171–178.
[35] Y.M. Liu, C.L. Hou, T.F. Jiao, et al., Nanomaterials 8 (2018) 35.
[36] Y. Feng, T.F. Jiao, J.J. Yin, et al., Nanoscale Res. Lett. 14 (2019) 78.
[37] J.L. Zhu, R. Wang, R. Geng, et al., RSC Adv. 9 (2019) 22551–22558.
[38] C.R. Wang, J.J. Yin, S.Q. Han, et al., Catalysts 9 (2019) 559.
[39] N. Hou, R. Wang, R. Geng, et al., Soft Matter 15 (2019) 6097–6106.
[40] S.W. Huo, P.F. Duan, T.F. Jiao, et al., Angew. Chem. Int. Ed. 56 (2017) 12174–12178.
[41] R. Guo, T.F. Jiao, R.F. Li, et al., ACS Sustain. Chem. Eng. 6 (2018) 1279–1288.
[42] K. Ma, W.J. Chen, T.F. Jiao, et al., Chem. Sci. 10 (2019) 6821–6827.
[43] Y. He, R. Wang, T.F. Jiao, et al., ACS Sustain. Chem. Eng. 7 (2019) 10888–10899.
[44] K.Y. Chen, T.F. Jiao, J.K. Li, et al., Langmuir 35 (2019) 3337–3345.
[45] K.Y. Chen, X.Y. Yan, J.K. Li, et al., Nanomaterials 9 (2019) 284.